THE JOURNAL OF PHYSICAL CHEMISTRY LETTERS
A JOURNAL OF THE AMERICAN CHEMICAL SOCIETY

pubs.acs.org/JPCL Letter

Infrared Spectroscopy of Stepwise Hydration Motifs of Sulfur Dioxide

Chong Wang,[#] Liangfei Fu,[#] Shuo Yang, Huijun Zheng, Tiantong Wang, Jiao Gao, Mingzhi Su, Jiayue Yang, Guorong Wu, Weiqing Zhang, Zhaojun Zhang,* Gang Li,* Dong H. Zhang, Ling Jiang,* and Xueming Yang

Cite This: J. Phys. Chem. Lett. 2022, 13, 5654−5659 Read Online

ABSTRACT: Experimental characterization of microscopic events and behaviors of SO_2-H_2O interactions is crucial to understanding SO_2 atmospheric chemistry but has been proven to be very challenging due to the difficulty in size selection. Here, size-dependent development of SO_2 hydrate structure and cluster growth in the $SO_2(H_2O)_n$ (n = 1−16) complexes was probed by infrared spectroscopy based on threshold photoionization using a tunable vacuum ultraviolet free electron laser. Spectral changes with cluster size demonstrate that the sandwich structure initially formed at n = 1 develops into cycle structures with the sulfur and oxygen atoms in a two-dimensional plane (n = 2 and 3) and then into three-dimensional cage structures ($n \geq 4$). SO_2 is favorably bound to the surface of larger water clusters. These stepwise features of SO_2 hydration on various sized water clusters contribute to understanding the reactive sites and electrophilicity of SO_2 on cloud droplets, which may have important atmospheric implications for studying the SO_2-containing aerosol systems.

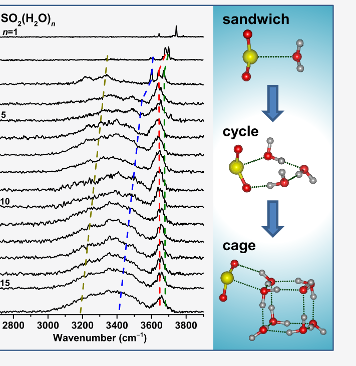

The interaction of atmospheric pollutants with the water surfaces plays a crucial role in atmospheric new particle formation, cloud formation, and climate change.[1−6] Sulfur dioxide (SO_2) is an important atmospheric pollutant and has been involved in many atmospheric processes such as the formation of cloud condensation nuclei and acid rain.[7−9] Characterizing the chemical composition, structure, and growth of nucleating precursors is essential in understanding the underlying mechanisms of atmospheric new particle formation.[10−12] The existence of SO_2 hydrate species with a $_{(SO2)}O\cdots H_{(H2O)}$ binding motif at the water surface was identified by vibrational sum-frequency generation (SFG) spectroscopy, whereas the $_{(SO2)}S\cdots O_{(H2O)}$ sandwich species was not observed.[13−16] Those authors rationalized this absence by considering the quick reaction of SO_2 with water. Recent comprehensive computational studies indicate that the dominant interaction between SO_2 and H_2O in the gas phase and on the water nanodroplet is $_{(SO2)}S\cdots O_{(H2O)}$ and $_{(SO2)}O\cdots H_{(H2O)}$, respectively.[17] Along with significant advances in theoretical calculations, these studies have provided great insights into the SO_2 solvation on aqueous surfaces.[18−25] In spite of extensive efforts, no direct experimental evidence has been obtained for size-dependent development of SO_2 hydrate structure and cluster growth. Such measurement of molecular cluster precursors is helpful for understanding the stepwise formation of atmospheric new particles, because different sizes of droplets exist during the aerosol nucleation and growth processes.[26]

Gaseous clusters have been subject to numerous spectroscopic investigations as ideal systems to get molecular-level insights into the structures of the solvation shells or the specific interactions between the solute and solvent molecules.[27−38] Infrared photodissociation spectroscopy of size-selected ionic clusters has been one of the most important methods for probing microscopic ion hydrations.[33−38] However, spectroscopic investigation of SO_2 hydration with neutral water clusters has been proven to be very challenging due to the difficulty in size selection of neutral clusters in general, except for the small-sized $SO_2(H_2O)_n$ (n = 1−3) clusters explored by matrix-isolation IR and microwave spectroscopy.[39−41] Very recently, we set up an IR spectroscopic facility based on threshold photoionization using a tunable vacuum ultraviolet free electron laser (VUV-FEL),[42−44] which allows for size selection of neutral clusters. With this new technique, the measurements of IR spectra of a wide variety of neutral clusters become possible.[45−47] Here, we report the size-specific IR spectroscopic signatures of neutral $SO_2(H_2O)_n$ (n = 1−16) clusters using a VUV-FEL-based IR spectroscopy. The spectra are analyzed with the help of simulated vibrational spectra from quantum chemical calculations. General trends in the

Received: May 15, 2022
Accepted: June 14, 2022

https://doi.org/10.1021/acs.jpclett.2c01472
J. Phys. Chem. Lett. 2022, 13, 5654−5659

stepwise hydration motifs of SO_2 are deduced from the reasonable agreement between the experimental and calculated spectra.

The IR spectra of $SO_2(H_2O)_n$ clusters were measured using a VUV-FEL-based IR spectroscopy apparatus (see the Supporting Information for experimental details).[42] Neutral $SO_2(H_2O)_n$ clusters were generated by supersonic expansions of SO_2-H_2O/helium mixtures using a high-pressure pulsed valve. For the IR excitation of neutral $SO_2(H_2O)_n$ clusters, we used a tunable IR optical parametric oscillator/amplifier system (LaserVision). Subsequent photoionization was carried out with about 30 ns delay with a VUV-FEL light. When the VUV threshold photoionization does not cause the cluster fragmentation, a mass-selective IR spectrum of a given $SO_2(H_2O)_n$ cluster can be observed as a decrease of signal intensity of the $SO_2(H_2O)_n^+$ cation as a function of IR wavelength. Various experimental conditions (the wavelength and pulse energy of VUV-FEL, the concentration of SO_2-H_2O/helium mixture, and the stagnation pressure, etc.) were optimized to maximize the signal of a size-specific cluster of interest with no interference from larger clusters. IR power dependence of the signal was measured to ensure that the predissociation yield was linear with photon flux.

The experimental IR spectra of $SO_2(H_2O)_n$ (n = 1−16) in the OH stretching region are shown in Figure 1a and band positions are listed in Table 1. The IR spectrum for n = 1 shows two main absorptions at 3643 and 3745 cm^{-1}, which are slightly red-shifted by 14 and 11 cm^{-1} from the symmetric (3657 cm^{-1}) and antisymmetric (3756 cm^{-1}) OH stretching vibrational frequencies of the free water molecule, respectively,

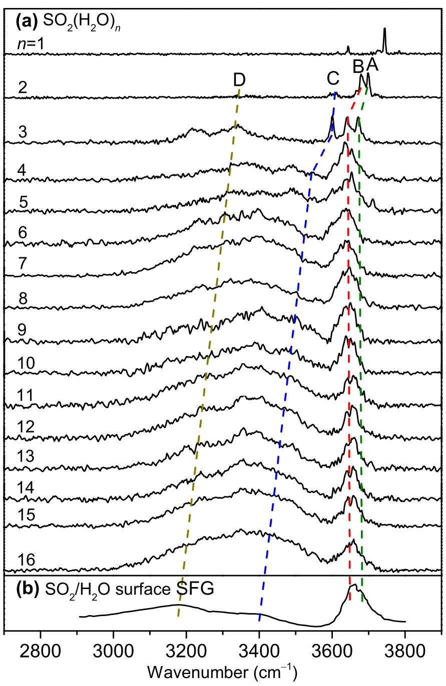

Figure 1. Experimental IR spectra of the $SO_2(H_2O)_n$ (n = 1−16) clusters (a). The SFG spectrum of SO_2 gas at the vapor/water surface at 273 K is shown at the bottom (b).[13] The OH stretch fundamentals assigned to free OH stretch of water bound to water (A) (green dash line), OH stretch of water in the $_{(SO2)}O\cdots H_{(H2O)}$ interaction (B) (red dash line), OH stretch of water in the $_{(SO2)}S\cdots O_{(H2O)}$ interaction (C) (blue dash line), and hydrogen-bonded OH stretch of water bound to water (D) (dark yellow dash line) are indicated.

reflecting a gentle softening of these modes upon SO_2 hydration as bonding electron density is withdrawn from the water molecule.[48] In the IR spectrum for n = 2, two intense bands at 3699 (labeled A) and 3679 (labeled B) cm^{-1} and weak bands centered at 3611 (labeled C) and 3361 (labeled D) cm^{-1} are observed. Band D gains some intensities in the spectrum of n = 3. Starting at n = 4, bands A and B are merged to a broad feature centered at 3675 and 3635 cm^{-1}, respectively; band C is broadened and coupled with band D to spread out in the 3000−3635 cm^{-1} region. The frequencies of these bands do not vary appreciably with the increase of cluster size, but rather, the observable effect is a variation of the intensity distribution of bands C and D.

To understand the experimental IR spectra and identify the structures of the $SO_2(H_2O)_n$ clusters, quantum chemical calculations were carried out (see the Supporting Information for theoretical details). Because of computational limitations, only the n = 1−8 clusters were studied theoretically. The structures were obtained using the constrained basin-hopping global minimum search.[49] The geometries and energies for the low-lying structures were refined at the MP2/aug-cc-pVDZ (AVDZ) level of theory. Note that many nearly isoenergetic isomers might contribute to the present IR spectra, but only a few lowest-lying structures (Figure 2) were selected to gain insight into the structural and spectral evolution. For n = 1−6, the anharmonic vibrational spectra were calculated using the anharmonic quantum simulation method based on the full-dimensional *ab initio* potential energy surface. For n = 7 and 8, which degrees of freedom are too large to be precisely described by the anharmonic quantum simulations, their harmonic vibrational spectra were calculated at the MP2/AVDZ level of theory. The total vibrational spectra were calculated as the population weighted average of the contributions from the representative structures at finite temperature. Although it is cumbersome to estimate the experimental temperature of $SO_2(H_2O)_n$ clusters, the rotational temperature should be less than 10 K, while the vibrational temperature could be much higher (i.e., a finite temperature), because vibrations are not easily cooled as rotations in the supersonic expansions.[45] The calculated IR spectra at the more atmospherically relevant cold temperature of 200 K[22] are used for the present discussions, which are shown in Figure 3. The comparison of calculated and experimental spectra for each cluster is given in Figures S1−S8, respectively.

For the n = 1 cluster, the lowest-energy isomer (Figure 2, labeled 1-I) is a "sandwich" type structure with a $_{(SO2)}S\cdots O_{(H2O)}$ binding motif, which is consistent with previous matrix-isolation IR and microwave spectroscopic and theoretical results.[19,22,23,39−41,50] The 1-II isomer consists of a $_{(SO2)}O\cdots H_{(H2O)}$ binding motif, which lies 1.57 kcal/mol higher in energy than 1-I. As shown in Table S1, the population of isomer 1-I at 200 K is 98.7%, suggesting that 1-I should be the main isomer present at finite temperature. As shown in Figure S1, the calculated band positions and relative intensities of the symmetric (3643 cm^{-1}) and antisymmetric (3736 cm^{-1}) OH stretches are in excellent agreement with the experimental values.

For the n = 2 cluster, the lowest-energy isomer (Figure 2, part 2-I) is a cyclic hydrate structure with one $_{(SO2)}S\cdots O_{(H2O)}$ bond, one $_{(SO2)}O\cdots H_{(H2O)}$ bond, and one water−water hydrogen bond (H-bond).[19,22,23,39−41,50] The 2-II and 2-III isomers have a similar ring arrangement with the difference in

https://doi.org/10.1021/acs.jpclett.2c01472
J. Phys. Chem. Lett. 2022, 13, 5654−5659

Table 1. Experimental Vibrational Frequencies (cm^{-1}) and Band Assignments for $SO_2(H_2O)_n$ (n = 1−16)

label	n = 1	n = 2	n = 3	n = 4−16	assignment
A	–	3699	3671	3675	free OH stretch of water bound to water (OH_W^{free})
B	–	3679	3641	3635	OH stretch of water in the $_{(SO2)}O\cdots H_{(H2O)}$ interaction ($OH_S^{SO\cdots HO}$)
C	3745 3643	3611	3601	3300−3580	OH stretch of water in the $_{(SO2)}S\cdots O_{(H2O)}$ interaction ($OH_S^{OS\cdots OH}$)
D	–	3361	3100−3430	3000−3300	hydrogen-bonded OH stretch of water bound to water (OH_W^{HB})

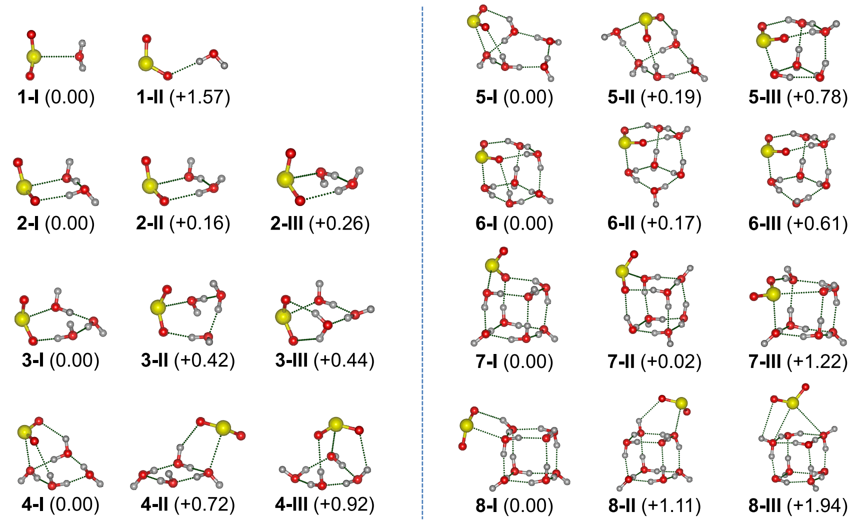

Figure 2. Representative low-lying structures of $SO_2(H_2O)_n$ (n = 1−8) (S, yellow; O, red; H, light gray). The calculations were performed at the MP2/AVDZ level of theory. Relative energies (in kcal/mol) are listed inside round brackets.

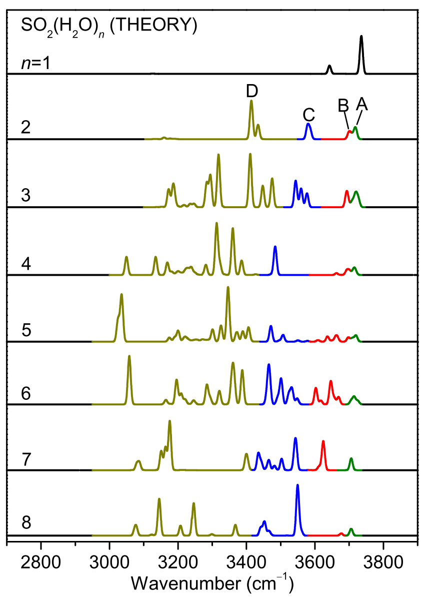

Figure 3. Total weighted vibrational spectra of $SO_2(H_2O)_n$ (n = 1−8). The anharmonic vibrational spectra of the n = 1−6 clusters were calculated using the anharmonic quantum simulation method based on the full-dimensional ab initio potential energy surface, and the harmonic vibrational spectra of the n = 7 and 8 clusters were calculated at the MP2/AVDZ level of theory.

the orientation of the hydrogen atom. In the calculated IR spectra (Figure S2), band A (3718 cm^{-1}) and band B (3701 cm^{-1}) is due to the free OH stretch of water bound to water (OH_W^{free}) and the OH stretch of water in the $_{(SO2)}O\cdots H_{(H2O)}$ interaction ($OH_S^{SO\cdots HO}$), respectively, consistent with the experimental values (3699 and 3679 cm^{-1}); band C (3580 cm^{-1}) is attributed to the OH stretch of water in the $_{(SO2)}S\cdots O_{(H2O)}$ interaction ($OH_S^{OS\cdots OH}$). The sharp bands centered at 3415 cm^{-1} (labeled D, H-bonded OH stretch of water bound to water (OH_W^{HB})) are smeared out in the experimental spectrum, which could be rationalized by the dynamic fluctuations of H-bonds as demonstrated in various hydrated clusters.[28,31,33−38] The calculated relative intensities are less satisfactory in agreement with the experimental ones, which might be due to the complexity of experiment (IR absorption mechanism, saturation effects, etc.) or to the limitation of theoretical calculations (neglected degrees of freedom or limited sampling of the potential energy surface, etc.).[51,52]

The lowest-energy isomer for n = 3 (Figure 2, 3-I) also consists of a cyclic hydrate structure with one $_{(SO2)}S\cdots O_{(H2O)}$ bond, one $_{(SO2)}O\cdots H_{(H2O)}$ bond, and two water−water H-bonds. The 3-II structure (+0.42 kcal/mol) is similar to that of 3-I. The 3-III isomer (+0.44 kcal/mol) contains one $_{(SO2)}S\cdots O_{(H2O)}$ bond, two $_{(SO2)}O\cdots H_{(H2O)}$ bonds, and two water−water H-bonds. It can be seen from Table S1 that 3-I is dominant at ≤200 K, which is consistent with previous *ab initio* molecular dynamics simulations.[22] As shown in Figure S3, the total IR spectra of the 3-I, 3-II, and 3-III isomers reproduce the experimental spectrum better. The calculated position of band C is red-shifted from the experimental value. As compared to n = 2, the calculated band D contains more peaks, which would enhance the band intensities as illustrated in the experimental spectrum.

For the n = 4 cluster, all the three lowest-energy isomers have a similar four-membered water ring (Figure 2), in which each water molecule donates one hydrogen atom to form a single H-bond with an adjacent water molecule. The SO_2 molecule is bonded to different sites of this ring, forming the

https://doi.org/10.1021/acs.jpclett.2c01472
J. Phys. Chem. Lett. 2022, 13, 5654−5659

$_{(SO2)}$S···O$_{(H2O)}$ and $_{(SO2)}$O···H$_{(H2O)}$ interactions. The 4-II isomer is dominant at 200 K (Table S1). The total IR spectrum is in reasonable agreement with the experimental one (Figure S4).

For the n = 5 cluster, the 5-I isomer has a five-membered water ring, similar to the arrangement in 4-I. The 5-II isomer consists of a cage structure with a four-membered water ring. The 5-III isomer contains a prism-like structure. In the n = 6 cluster, a cuboidal structure is favorably formed in the 6-I isomer, while one $_{(SO2)}$O···H$_{(H2O)}$ bond of such motif is broken in the 6-II and 6-III isomers. In the n = 7 cluster, the SO_2 molecule is bonded to the corner of the water cage. In the n = 8 cluster, the SO_2 molecule is bonded to the outer side of the cuboidal water octamer. Overall, good agreement between the experimental and simulated vibrational spectra (Figures S5−S8) indicates that the n-I (n = 5−8) isomers are the main structures present in the experiment.

The structures and IR spectra of the hydrolysis products ($H_2SO_3(H_2O)_{n-1}$) were calculated for n = 1−6, and the results are shown in Figure S9. It is found that the $H_2SO_3(H_2O)_{n-1}$ species lie higher in energy than $SO_2(H_2O)_n$ and such relative energy decreases with the increasing number of water molecules. The calculated IR spectra of $H_2SO_3(H_2O)_{n-1}$ show distinct OH stretch peaks, which are not observed experimentally. It thus appears that the hydrolysis reaction of SO_2 in small water clusters is unfavorable. These results are consistent with the previous prediction of a considerable energy barrier for the SO_2 + $(H_2O)_5$ reaction (5.69 kcal/mol).[23]

Although the selection rules for IR activity of hydrated clusters are different from those at play in the vibrational SFG of aqueous surface, it is useful to compare the vibrational patterns, with representative SFG spectra of SO_2/H_2O interface presented in Figure 1b. In the SFG spectra, bands A, B, C, and D were assigned to the free OH stretches, the OH stretches of SO_2:H_2O surface complex, and the topmost and the deeper interfacial OH stretches, respectively.[13−16,20] As shown in Figure 1, the frequencies of the observed absorption bands in the cluster spectra shift toward their aqueous values as the number of water molecule is increased. The major difference between the cluster spectra and the interface SFG spectra is the intensities of bands C and D, which might be due to the fact that the water clusters are not sufficiently big to represent the H-bond networks of liquid water.

The frequency shifts observed in the IR spectra as a function of cluster size are reasonably reproduced by the calculations (Figure 3), which allows us to determine general trends in the stepwise hydration motifs of SO_2. As summarized in Figure 4, the sandwich structure initially formed at n = 1 develops into cycle structures with the sulfur and oxygen atoms in a two-dimensional plane (n = 2 and 3), and then into three-dimensional cage structures ($n \geq 4$). The most important of these motifs is the strong preference of the binding of SO_2 on the outer side of the water clusters.

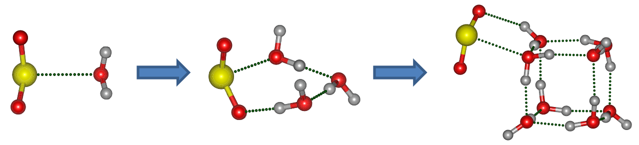

Figure 4. Schematic representation of the development of hydrogen-bond network structure with increasing cluster size. (A) Sandwich structure in n = 1. (B) Two-dimensional cycle structure (n = 2 and 3). (C) Three-dimensional cage structure in $n \geq 4$.

It would be interesting to assess how the SO_2 adsorption alters the structures of water clusters. Previous studies indicated that the lowest-energy isomers of $(H_2O)_n$ (n = 3−5) have cyclic structures with all oxygen atoms in a two-dimensional (2D) plane, that of n = 6 and 7 has a 3D prism and prism-like structure, respectively, and that of n = 8 has a nominally cubic structure.[45,46,51−59] As shown in Figure 2, in the $SO_2(H_2O)_2$ cluster, the orientation of hydrogen atoms is tuned to bind with SO_2 to form a cyclic structure. In the $SO_2(H_2O)_3$ cluster, the ring of the water trimer is opened upon the SO_2 adsorption. The structures of the water tetramer and pentamer are kept during the uptake of SO_2. While the prism structures of the water hexamer and heptamer are broken, the pseudocubic structure of the water octamer remains. It could be estimated that the structures of larger water clusters might be slightly changed by the SO_2 adsorption. Indeed, the MP2/AVDZ calculated binding energies of SO_2 with water suggest that the n = 7 cluster may be a critical size of $SO_2(H_2O)_n$ complex to be stable (Table S2). The interaction motif between SO_2 and H_2O evolves from $_{(SO2)}$S···O$_{(H2O)}$ to $_{(SO2)}$O···H$_{(H2O)}$, which supports the proposed conversion of the dominant interaction in the gas phase and water nanodroplet.[17] Since the structures of hydrated SO_2 can affect the reactive sites and electrophilicity of SO_2,[17] the present cluster perspectives would aid our understanding of the solvation behaviors of SO_2 on the water nanodroplets and surfaces,[13−17,20,22,24]

In summary, infrared spectra are reported for the neutral $SO_2(H_2O)_n$ (n = 1−16) clusters in the 2700−3900 cm^{-1} spectral region. Quantum chemical calculations have been performed on the n = 1−8 clusters to identify the low-lying isomers and to assign the experimental spectral features. It is found that the sandwich structure initially formed at n = 1 develops into cycle structures with the sulfur and oxygen atoms in a two-dimensional plane (n = 2 and 3) and then into three-dimensional cage structures ($n \geq 4$) with the binding of SO_2 on the outer side of water clusters. Such consistent microscopic pictures have not previously been experimentally identified for the SO_2 binding to various sized water clusters. It is hoped that these results will both help to refine the SO_2−water intermolecular potentials to understand the macroscopic properties of SO_2 in the atmosphere and help to stimulate further studies of size-dependent solvation of many other gas molecules.

■ ASSOCIATED CONTENT

Supporting Information

The Supporting Information is available free of charge at https://pubs.acs.org/doi/10.1021/acs.jpclett.2c01472.

Experimental and theoretical methods, Figures S1−S9, Tables S1 and S2, references, and coordinates of the isomers (PDF)

Transparent Peer Review report available (PDF)

■ AUTHOR INFORMATION

Corresponding Authors

Zhaojun Zhang − *State Key Laboratory of Molecular Reaction Dynamics, Dalian Institute of Chemical Physics, Chinese*

https://doi.org/10.1021/acs.jpclett.2c01472
J. Phys. Chem. Lett. 2022, 13, 5654−5659

Academy of Sciences, Dalian 116023, China; orcid.org/0000-0002-4263-1789; Email: zhangzhj@dicp.ac.cn

Gang Li – *State Key Laboratory of Molecular Reaction Dynamics, Dalian Institute of Chemical Physics, Chinese Academy of Sciences, Dalian 116023, China;* orcid.org/0000-0001-5984-111X; Email: gli@dicp.ac.cn

Ling Jiang – *State Key Laboratory of Molecular Reaction Dynamics, Dalian Institute of Chemical Physics, Chinese Academy of Sciences, Dalian 116023, China; Hefei National Laboratory, Hefei 230088, China;* orcid.org/0000-0002-8485-8893; Email: ljiang@dicp.ac.cn

Authors

Chong Wang – *State Key Laboratory of Molecular Reaction Dynamics, Dalian Institute of Chemical Physics, Chinese Academy of Sciences, Dalian 116023, China; University of Chinese Academy of Sciences, Beijing 100049, China*

Liangfei Fu – *State Key Laboratory of Molecular Reaction Dynamics, Dalian Institute of Chemical Physics, Chinese Academy of Sciences, Dalian 116023, China; University of Chinese Academy of Sciences, Beijing 100049, China*

Shuo Yang – *State Key Laboratory of Molecular Reaction Dynamics, Dalian Institute of Chemical Physics, Chinese Academy of Sciences, Dalian 116023, China*

Huijun Zheng – *State Key Laboratory of Molecular Reaction Dynamics, Dalian Institute of Chemical Physics, Chinese Academy of Sciences, Dalian 116023, China; University of Chinese Academy of Sciences, Beijing 100049, China;* orcid.org/0000-0003-2876-7580

Tiantong Wang – *State Key Laboratory of Molecular Reaction Dynamics, Dalian Institute of Chemical Physics, Chinese Academy of Sciences, Dalian 116023, China; University of Chinese Academy of Sciences, Beijing 100049, China*

Jiao Gao – *State Key Laboratory of Molecular Reaction Dynamics, Dalian Institute of Chemical Physics, Chinese Academy of Sciences, Dalian 116023, China*

Mingzhi Su – *State Key Laboratory of Molecular Reaction Dynamics, Dalian Institute of Chemical Physics, Chinese Academy of Sciences, Dalian 116023, China; University of Chinese Academy of Sciences, Beijing 100049, China*

Jiayue Yang – *State Key Laboratory of Molecular Reaction Dynamics, Dalian Institute of Chemical Physics, Chinese Academy of Sciences, Dalian 116023, China*

Guorong Wu – *State Key Laboratory of Molecular Reaction Dynamics, Dalian Institute of Chemical Physics, Chinese Academy of Sciences, Dalian 116023, China;* orcid.org/0000-0002-0212-183X

Weiqing Zhang – *State Key Laboratory of Molecular Reaction Dynamics, Dalian Institute of Chemical Physics, Chinese Academy of Sciences, Dalian 116023, China*

Dong H. Zhang – *State Key Laboratory of Molecular Reaction Dynamics, Dalian Institute of Chemical Physics, Chinese Academy of Sciences, Dalian 116023, China; Hefei National Laboratory, Hefei 230088, China*

Xueming Yang – *State Key Laboratory of Molecular Reaction Dynamics, Dalian Institute of Chemical Physics, Chinese Academy of Sciences, Dalian 116023, China; Hefei National Laboratory, Hefei 230088, China; Department of Chemistry, Southern University of Science and Technology, Shenzhen 518055, China;* orcid.org/0000-0001-6684-9187

Complete contact information is available at: https://pubs.acs.org/10.1021/acs.jpclett.2c01472

Author Contributions

[#]C.W. and L.F. contributed equally to this work.

Notes

The authors declare no competing financial interest.

■ ACKNOWLEDGMENTS

The authors gratefully acknowledge the Dalian Coherent Light Source (DCLS) and Specreation Co., Ltd., for support and assistance. This work was supported by the National Natural Science Foundation of China (22125303, 92061203, 22173097, 22103082, and 21688102), the National Key Research and Development Program of China (2021YFA1400501), the Innovation Program for Quantum Science and Technology (2021ZD0303304), the Strategic Priority Research Program of the Chinese Academy of Sciences (CAS) (XDB17000000), the Dalian Institute of Chemical Physics (DICP DCLS201701), and the K. C. Wong Education Foundation (GJTD-2018-06).

■ REFERENCES

(1) Charlson, R. J.; Schwartz, S. E.; Hales, J. M.; Cess, R. D.; Coakley, J. A.; Hansen, J. E.; Hofmann, D. J. Climate Forcing by Anthropogenic Aerosols. *Science* **1992**, *255*, 423–430.

(2) Molina, M. J.; Molina, L. T.; Kolb, C. E. Gas-Phase and Heterogeneous Chemical Kinetics of the Troposphere and Stratosphere. *Annu. Rev. Phys. Chem.* **1996**, *47*, 327–367.

(3) Knipping, E. M.; Lakin, M. J.; Foster, K. L.; Jungwirth, P.; Tobias, D. J.; Gerber, R. B.; Dabdub, D.; Finlayson-Pitts, B. J. Experiments and Simulations of Ion-Enhanced Interfacial Chemistry on Aqueous NaCl Aerosols. *Science* **2000**, *288*, 301–306.

(4) Davidovits, P.; Kolb, C. E.; Williams, L. R.; Jayne, J. T.; Worsnop, D. R. Mass Accommodation and Chemical Reactions at Gas-Liquid Interfaces. *Chem. Rev.* **2006**, *106*, 1323–1354.

(5) Garrett, B. C.; Schenter, G. K.; Morita, A. Molecular Simulations of the Transport of Molecules Across the Liquid/Vapor Interface of Water. *Chem. Rev.* **2006**, *106*, 1355–1374.

(6) von Schneidemesser, E.; et al. Chemistry and the Linkages between Air Quality and Climate Change. *Chem. Rev.* **2015**, *115*, 3856–3897.

(7) Hewitt, C. N. The Atmospheric Chemistry of Sulphur and Nitrogen in Power Station Plumes. *Atmos. Environ.* **2001**, *35*, 1155–1170.

(8) Sipila, M.; et al. The Role of Sulfuric Acid in Atmospheric Nucleation. *Science* **2010**, *327*, 1243–1246.

(9) Brandt, C.; Vaneldik, R. Transition Metal-Catalyzed Oxidation of Sulfur(IV) Oxides. Atmospheric-Relevant Processes and Mechanisms. *Chem. Rev.* **1995**, *95*, 119–190.

(10) Kolb, C. E.; Worsnop, D. R. Chemistry and Composition of Atmospheric Aerosol Particles. *Annu. Rev. Phys. Chem.* **2012**, *63*, 471–491.

(11) Sipila, M.; et al. Molecular-Scale Evidence of Aerosol Particle Formation via Sequential Addition of HIO_3. *Nature* **2016**, *537*, 532–534.

(12) Hu, J. H.; Shi, Q.; Davidovits, P.; Worsnop, D. R.; Zahniser, M. S.; Kolb, C. E. Reactive Uptake of Cl_2(g) and Br_2Cg) by Aqueous Surfaces as a Function of Br^- and I^- Ion Concentration: The Effect of Chemical Reaction at the Interface. *J. Phys. Chem.* **1995**, *99*, 8768–8776.

(13) Tarbuck, T. L.; Richmond, G. L. SO_2:H_2O Surface Complex Found at the Vapor/Water Interface. *J. Am. Chem. Soc.* **2005**, *127*, 16806–16807.

(14) Tarbuck, T. L.; Richmond, G. L. Adsorption and Reaction of CO_2 and SO_2 at a Water Surface. *J. Am. Chem. Soc.* **2006**, *128*, 3256–3267.

(15) Ota, S. T.; Richmond, G. L. Chilling Out: A Cool Aqueous Environment Promotes the Formation of Gas-Surface Complexes. *J. Am. Chem. Soc.* **2011**, *133*, 7497–7508.

(16) Ota, S. T.; Richmond, G. L. Uptake of SO_2 to Aqueous Dormaldehyde Surfaces. *J. Am. Chem. Soc.* **2012**, *134*, 9967−9977.
(17) Zhong, J.; Zhu, C.; Li, L.; Richmond, G. L.; Francisco, J. S.; Zeng, X. C. Interaction of SO_2 with the Surface of a Water Nanodroplet. *J. Am. Chem. Soc.* **2017**, *139*, 17168−17174.
(18) Li, W. K.; McKee, M. L. Theoretical Study of OH and H_2O Addition to SO_2. *J. Phys. Chem. A* **1997**, *101*, 9778−9782.
(19) Steudel, R.; Steudel, Y. Sulfur Dioxide and Water: Structures and Energies of the Hydrated Species SO_2-$n$$H_2O$, $[HSO_3]^-$-$n$$H_2O$, $[SO_3H]^-$-$n$$H_2O$, and H_2SO_3-$n$$H_2O$ (n = 0−8). *Eur. J. Inorg. Chem.* **2009**, *2009*, 1393−1405.
(20) Baer, M.; Mundy, C. J.; Chang, T.-M.; Tao, F.-M.; Dang, L. X. Interpreting Vibrational Sum-Frequency Spectra of Sulfur Dioxide at the Air/Water Interface: A Comprehensive Molecular Dynamics Study. *J. Phys. Chem. B* **2010**, *114*, 7245−7249.
(21) Tachikawa, H. Collision Induced Complex Formation following Electron Capture of SO_2-H_2O Complex Interacting with Argon Atoms. *J. Phys. Chem. A* **2011**, *115*, 9091−9096.
(22) Shamay, E. S.; Valley, N. A.; Moore, F. G.; Richmond, G. L. Staying Hydrated: The Molecular Journey of Gaseous Sulfur Dioxide to a Water Surface. *Phys. Chem. Chem. Phys.* **2013**, *15*, 6893−6902.
(23) Liu, J.; Fang, S.; Liu, W.; Wang, M.; Tao, F.-M.; Liu, J.-Y. Mechanism of the Gaseous Hydrolysis Reaction of SO_2: Effects of NH_3 versus H_2O. *J. Phys. Chem. A* **2015**, *119*, 102−111.
(24) Zhong, J.; Kumar, M.; Anglada, J. M.; Martins-Costa, M. T. C.; Ruiz-Lopez, M. F.; Zeng, X. C.; Francisco, J. S. Atmospheric Spectroscopy and Photochemistry at Environmental Water Interfaces. *Annu. Rev. Phys. Chem.* **2019**, *70*, 45−69.
(25) Misiewicz, J. P.; Moore, K. B., III; Franke, P. R.; Morgan, W. J.; Turney, J. M.; Douberly, G. E.; Schaefer, H. F., III Sulfurous and Sulfonic Acids: Predicting the Infrared Spectrum and Setting the Surface Straight. *J. Chem. Phys.* **2020**, *152*, 024302.
(26) Zhang, R.; Khalizov, A.; Wang, L.; Hu, M.; Xu, W. Nucleation and Growth of Nanoparticles in the Atmosphere. *Chem. Rev.* **2012**, *112*, 1957−2011.
(27) Zwier, T. S. The Spectroscopy of Solvation in Hydrogen-Bonded Aromatic Clusters. *Annu. Rev. Phys. Chem.* **1996**, *47*, 205−241.
(28) Buck, U.; Huisken, F. Infrared Spectroscopy of Size-Selected Water and Methanol Clusters. *Chem. Rev.* **2000**, *100*, 3863−3890.
(29) Keutsch, F. N.; Saykally, R. J. Water Clusters: Untangling the Mysteries of the Liquid, One Molecule at a Time. *Proc. Natl. Acad. Sci. U. S. A.* **2001**, *98*, 10533−10540.
(30) Wang, X.-B.; Wang, L.-S. Photoelectron Spectroscopy of Multiply Charged Anions. *Annu. Rev. Phys. Chem.* **2009**, *60*, 105−126.
(31) Heine, N.; Asmis, K. R. Cryogenic Ion Trap Vibrational Spectroscopy of Hydrogen-Bonded Clusters Relevant to Atmospheric Chemistry. *Int. Rev. Phys. Chem.* **2015**, *34*, 1−34.
(32) Weichman, M. L.; Neumark, D. M. Slow Photoelectron Velocity-Map Imaging of Cryogenically Cooled Anions. *Annu. Rev. Phys. Chem.* **2018**, *69*, 101−124.
(33) Ebata, T.; Fujii, A.; Mikami, N. Vibrational Spectroscopy of Small-Sized Hydrogen-Bonded Clusters and Their Ions. *Int. Rev. Phys. Chem.* **1998**, *17*, 331−361.
(34) Duncan, M. A. Frontiers in the Spectroscopy of Mass-Selected Molecular Ions. *Int. J. Mass Spectrom.* **2000**, *200*, 545−569.
(35) Bieske, E. J.; Dopfer, O. High-Resolution Spectroscopy of Cluster Ions. *Chem. Rev.* **2000**, *100*, 3963−3998.
(36) Robertson, W. H.; Johnson, M. A. Molecular Aspects of Halide Ion Hydration: The Cluster Approach. *Annu. Rev. Phys. Chem.* **2003**, *54*, 173−213.
(37) Asmis, K. R.; Neumark, D. M. Vibrational Spectroscopy of Microhydrated Conjugate Base Anions. *Acc. Chem. Res.* **2012**, *45*, 43−52.
(38) Yang, N.; Duong, C. H.; Kelleher, P. J.; McCoy, A. B.; Johnson, M. A. Deconstructing Water's Diffuse OH Stretching Vibrational Spectrum with Cold Clusters. *Science* **2019**, *364*, 275−278.
(39) Schriver, A.; Schriver, L.; Perchard, J. P. Infrared Matrix Isolation Studies of Complexes between Water and Sulfur Dioxide: Identification and Structure of the l:l, 1:2, and 2:l Species. *J. Mol. Spectrosc.* **1988**, *127*, 125−142.
(40) Hirabayashi, S.; Ito, F.; Yamada, K. M. T. Infrared Spectra of the $(H_2O)_n$-SO_2 Complexes in Argon Matrices. *J. Chem. Phys.* **2006**, *125*, 034508.
(41) Matsumura, K.; Lovas, F. J.; Suenram, R. D. The Microwave Spectrum and Structure of the H_2O-SO_2 Complex. *J. Chem. Phys.* **1989**, *91*, 5887−5894.
(42) Zhang, B.; et al. Infrared Spectroscopy of Neutral Water Dimer Based on a Tunable Vacuum Ultraviolet Free Electron Laser. *J. Phys. Chem. Lett.* **2020**, *11*, 851−855.
(43) Li, G.; et al. Infrared plus Vacuum Ultraviolet Two-Color Ionization Spectroscopy of Neutral Metal Complexes based on a Tunable Vacuum Ultraviolet Free-Electron Laser. *Rev. Sci. Instrum.* **2020**, *91*, 034103.
(44) Li, G.; Wang, C.; Zheng, H.-J.; Wang, T.-T.; Xie, H.; Yang, X.-M.; Jiang, L. Infrared Spectroscopy of Neutral Clusters based on a Vacuum Ultraviolet Free Electron Laser. *Chin. J. Chem. Phys.* **2021**, *34*, 51−60.
(45) Zhang, B.; et al. Infrared Spectroscopy of Neutral Water Clusters at Finite Temperature: Evidence for a Noncyclic Pentamer. *Proc. Natl. Acad. Sci. U. S. A.* **2020**, *117*, 15423−15428.
(46) Li, G.; et al. Infrared Spectroscopic Study of Hydrogen Bonding Topologies in the Smallest Ice Cube. *Nat. Commun.* **2020**, *11*, 5449.
(47) Jiang, S.; et al. Vibrational Signature of Dynamic Coupling of a Strong Hydrogen Bond. *J. Phys. Chem. Lett.* **2021**, *12*, 2259−2265.
(48) Vaden, T. D.; Weinheimer, C. J.; Lisy, J. M. Evaporatively Cooled $M^+(H_2O)Ar$ Cluster Ions: Infrared Spectroscopy and Internal Energy Simulations. *J. Chem. Phys.* **2004**, *121*, 3102−3107.
(49) Chen, X.; Zhao, Y.-F.; Wang, L.-S.; Li, J. Recent Progresses of Global Minimum Searches of Nanoclusters with a Constrained Basin-Hopping Algorithm in the TGMin Program. *Comput. Theor. Chem.* **2017**, *1107*, 57−65.
(50) Bishenden, E.; Donaldson, D. J. Ab Initio Study of $SO_2 + H_2O$. *J. Phys. Chem. A* **1998**, *102*, 4638−4642.
(51) Buck, U.; Ettischer, I.; Melzer, M.; Buch, V.; Sadlej, J. Structure and Spectra of Three-Dimensional $(H_2O)_n$ Clusters, n = 8, 9, 10. *Phys. Rev. Lett.* **1998**, *80*, 2578−2581.
(52) Cole, W. T. S.; Farrell, J. D.; Wales, D. J.; Saykally, R. J. Structure and Torsional Dynamics of the Water Octamer from THz Laser Spectroscopy near 215 μm. *Science* **2016**, *352*, 1194−1197.
(53) Pugliano, N.; Saykally, R. J. Measurement of Quantum Tunneling Between Chiral Isomers of the Cyclic Water Trimer. *Science* **1992**, *257*, 1937−1940.
(54) Cruzan, J. D.; Braly, L. B.; Liu, K.; Brown, M. G.; Loeser, J. G.; Saykally, R. J. Quantifying Hydrogen Bond Booperativity in Water: VRT Spectroscopy of the Water Tetramer. *Science* **1996**, *271*, 59−62.
(55) Liu, K.; Brown, M. G.; Cruzan, J. D.; Saykally, R. J. Vibration-Rotation Tunneling Spectra of the Water Pentamer: Structure and Dynamics. *Science* **1996**, *271*, 62−64.
(56) Pribble, R. N.; Zwier, T. S. Size-Specific Infrared Spectra of Benzene-$(H_2O)_n$ Clusters (n = 1 through 7): Evidence for Noncyclic $(H_2O)_n$ Structures. *Science* **1994**, *265*, 75−79.
(57) Perez, C.; Muckle, M. T.; Zaleski, D. P.; Seifert, N. A.; Temelso, B.; Shields, G. C.; Kisiel, Z.; Pate, B. H. Structures of Cage, Prism, and Book Isomers of Water Hexamer from Broadband Rotational Spectroscopy. *Science* **2012**, *336*, 897−901.
(58) Brudermann, J.; Melzer, M.; Buck, U.; Kazimirski, J. K.; Sadlej, J.; Bush, V. The Asymmetric Cage Structure of $(H_2O)_7$ from a Combined Spectroscopic and Computational Study. *J. Chem. Phys.* **1999**, *110*, 10649−10652.
(59) Zhang, Y.-Y.; et al. Infrared Spectroscopic Signature of the Structural Diversity of the Water Heptamer. *Cell Rep. Phys. Sci.* **2022**, *3*, 100748.